

Indirect detection prospects for $d^*(2380)$ dark matter

Geoff Beck

School of Physics, University of the Witwatersrand, Private Bag 3, WITS-2050,
Johannesburg, South Africa

E-mail: geoffrey.beck@wits.ac.za

March 2020

Abstract. A Bose-Einstein condensate of the hexaquark particle known as $d^*(2380)$ has been recently proposed as a dark matter candidate by the authors in Bashkanov & Watts 2020. This particle can produced in an abundant condensate state in the early universe and is argued to satisfy all the stability and weak interaction constraints of a viable dark matter candidate. This dark matter candidate is able to evade direct detection bounds and is suggested to have the best observational prospects in the form of indirect astrophysical emissions due to the decay of the d^* condensate. In this work we test the indirect observational prospects of this form of dark matter and find that its low mass ~ 2 GeV mean that sub-GeV gamma-rays searches have the best prospects in the Milky-Way galactic centre where we find $\Gamma_{d^*} < 3.9 \times 10^{-24} \text{ s}^{-1}$, with current extra-galactic data from M31 and the Coma cluster producing constraints on the d^* decay rate two orders of magnitude weaker.

Keywords: dark matter, hexaquarks

Submitted to: *J. Phys. G: Nucl. Part. Phys.*

1. Introduction

The nature of Dark Matter (DM) remains one of the most important problems in astroparticle physics. Despite extensive gravitational evidence [1, 2, 3, 4, 5] (or see [6] for a review) neither direct [7] (or see [8] and references therein for a review) nor indirect searches [6, 9, 10, 11, 12, 13, 14, 15, 16, 17, 18, 19, 20, 21, 22, 23] have produced anything beyond parameter space constraints on models of cold (or non-relativistic at the time of freeze-out) DM normally favoured by the eponymous, and now standard, Λ CDM model of cosmology [1]. In particular direct detection experiments have strongly narrowed the space of viable supersymmetric Weakly Interacting Massive Particles (WIMPs) [7]. Other promising candidates such as sterile neutrinos are being actively searched for in both indirect and laboratory experiments, see [24] for a review. In addition, the axion

or axion-like-particle has been the subject of searches in multiple forms [25, 26, 27, 28]. Despite a variety of theoretically well-motivated candidates for a DM particle, and a wide array of on-going searches, no positive evidence has emerged in favour of any particular model. This makes the exploration of new ideas to explain the nature of DM both necessary and worthwhile. This work is designed to explore the recent proposal of a new form of light quark based DM. This consists of having the hexaquark particle $d^*(2380)$ formed in the early universe and existing until the present epoch in the form of a stable Bose-Einstein Condensate (BEC) [29]. This proposal is particularly interesting as, unlike the aforementioned DM candidates, d^* particles are not part of an extension of the standard model of particle physics. The authors of [29] argue that production of d^* particles, during the quark-gluon plasma to hadronic phase transition, would be copious enough to account for present inferred DM abundance [1] and that the condensate's interactions with other matter would be sufficiently weak to justify consideration as a DM candidate.

The authors in [29] further argue that the most probable signature of this form of DM is likely to come from astrophysical emissions from the decay of the d^* BEC. In this letter we explore the potential of indirect observations to detect the signatures of d^* decay in both radio and gamma-ray frequencies. This is done by leveraging similar techniques to those used in multi-frequency indirect searches for cold DM particles. The schematic of the idea being that if the consequences of the decay of a single d^* are known, then standard model particle yields from the decay can be used to compute the observable emissions in an astrophysical environment. This requires incorporating data as to the structure of a target DM halo where the decays take place as well as the astrophysical environment in the form of local gas densities and magnetic field strengths, both of which can influence emissions from bremsstrahlung, inverse-Compton scattering, and synchrotron radiation. We specifically explore concentrated DM halos as these environments would contain the largest particle abundances and thus have a larger rate of DM decays, thus making for more visible signatures.

In particular we will explore several halos as target environments: the Coma cluster of galaxies, the Milky-Way galactic centre (GC), the Reticulum II dwarf galaxy, and M31 or the Andromeda galaxy. All of these environments have been previously used/proposed as targets in indirect DM searches [18, 13, 22, 11, 9, 30, 17, 10, 14, 31] in a variety of frequency bands from radio to gamma-rays. Barring the Reticulum II dwarf galaxy, all of the chosen targets have been the subject of extensive astrophysical study and thus have relatively well characterised environments in terms of gas densities and magnetic field profiles [32, 33, 34, 35]. In addition to this, the structure of each of the DM halos has previously been explored in the literature [11, 36, 31, 10, 37, 38, 39] (and references therein).

For simplicity we assume the decay rate of d^* is a constant Γ_{d^*} , although it would in principle depend upon the nature of the interactions between cosmic-rays and the d^* BEC [29]. Our findings are that the best extra-galactic target constraint on the decay rate was from the M31 galaxy with $\Gamma_{d^*} < 10^{-22} \text{ s}^{-1}$ which corresponds to lower limit on

the d^* BEC lifetime several orders of magnitude longer than the age of the universe [1]. A model independent search in diffuse galactic gamma-rays from [40] found $\Gamma < 10^{-24} \text{ s}^{-1}$ but the photon yield per decay in this model exceeds the hexaquark case from [29] by 5 orders of magnitude at energies around 0.1 GeV where our constraints are derived. So we exceed a ‘model-translated’ version of the [40] limit by two orders of magnitude in extra-galactic targets. We also note that a very similar model independent limit to that of [40] is derived from reionisation effects in [41].

In our own galactic centre we find the strongest observational prospect. Using the CLUMPY software [37, 38, 39] to determine a dark matter halo density profile we find that $\Gamma_{d^*} < 3.9 \times 10^{-24}$, a full two order of magnitude improvement on extra-galactic data. The galactic centre gamma-ray data set we used was for the Fermi-LAT GeV excess spectrum from [30] as this d^* decay contributes to anomalous emissions not covered by the Fermi templates. The use of this spectrum greatly improves constraints as the flux is at least an order of magnitude below the total signal observed by Fermi-LAT. These limits better the translated limits from [40] by 5 orders of magnitude and are competitive with the unmodified limits on light DM decay via electrons with final-state radiation (we compare to this case as its spectral shape is most similar to the d^* data from [29]).

This letter is structured as follows: in section 2 the particle distribution functions from d^* decays are discussed followed by an examination of the emission mechanisms following d^* decay. The DM target halos and their observational data sets are described in 3. The results are presented and discussed in section 4 and conclusions are drawn and summarised in section 5.

2. The formalism for emissions from $d^*(2380)$ decay

The physical quantity of interest in indirect DM hunts is the flux of photons produced as consequence of the annihilation/decay of DM particles. In the case of the d^* we are interested only in the decay [29]. There are two forms of flux we are interested in and we will label them primary and secondary. Primary emissions result from the prompt production of photons, either directly as part of the decay products or radiation from the prompt decay of these products (and/or final state radiation). Secondary emissions result from the interaction of decay products with the astrophysical environment. Thus, these will consist of Inverse-Compton Scattering (ICS), bremsstrahlung, and synchrotron radiation. All of the secondary radiation studied will be sourced from electrons that result from the products of the d^* decay and thus the processes that affect the energy-loss and diffusion of electrons in astrophysical environments will also be discussed.

2.1. Primary emissions

The primary emission flux S_γ (photons per unit area per unit time) is simply calculated as follows

$$S_\gamma(\nu, r, z) = \int_0^r d^3r' \frac{Q_\gamma(\nu, z, r')}{4\pi(D_L^2 + (r')^2)} , \quad (1)$$

where this is the flux from within the volume bounded by radius r , D_L is the luminosity distance to the halo centre, and Q_γ is the gamma-ray source function from d^* decays.

The source function for particle species i following d^* decay is found according to

$$Q_i(r, E) = \Gamma_{d^*} \frac{dN_i}{dE} \left(\frac{\rho_{d^*}(r)}{m_{d^*}} \right) , \quad (2)$$

where Γ_{d^*} is the decay rate, $\frac{dN_i}{dE}$ is the particle number produced per unit energy from a d^* decay, $\rho_{d^*}(r)$ is the DM density (which will come from the structure of the DM halo), and $m_{d^*} = 2.380$ GeV. It is worth noting that [29] suggest that the condensate decay requires energy injection, via cosmic ray collisions with the d^* BEC for instance, this means that the decay rate is in principle the product of the local cosmic-ray density and the velocity averaged interaction cross-section $\langle\sigma v\rangle$ between the BEC and cosmic rays. In this work we will treat Γ_{d^*} as a universal constant for simplicity as the nature of the interactions between d^* and cosmic-rays are not specified in [29]. A full treatment will not invalidate the results presented here, rather it will clarify what limits result on $\langle\sigma v\rangle$. The yield functions $\frac{dN_i}{dE}$ are drawn from results presented in [29] with the possible decay modes being to photons (via neutral pions) and charged pions. Nucleons and deuterons are also considered in [29] but are not relevant in the context of this work. It is important to note that the authors in [29] present yields for π^\pm but not e^\pm , the latter being more relevant for astronomical signatures. Thus, to obtain the e^\pm yields, we convert the pion distributions to those of electrons/positrons following [42] which notably omits radiative corrections. An important caveat here is that a pure 6 quark state is assumed for the d^* particle by [29] whereas it is argued in the literature that it is likely to be an admixture of hadronic and quark states [43]. This may have implications on the particle source function that cannot be immediately quantified.

2.2. Electron equilibrium distributions

Secondary emission mechanisms require the spectrum of electrons injected via DM decays. These electrons lose energy through radiation and diffuse from their original point of injection. Thus, their distribution when considering long emission time-scales (as appropriate in astrophysical scenarios) will be taken to be the equilibrium solution to the diffusion-loss equation

$$\frac{\partial}{\partial t} \frac{dn_e}{dE} = \nabla \cdot \left(D(E, \mathbf{r}) \nabla \frac{dn_e}{dE} \right) + \frac{\partial}{\partial E} \left(b(E, \mathbf{r}) \frac{dn_e}{dE} \right) + Q_e(E, \mathbf{r}) . \quad (3)$$

where Q_e is the electron source function from d^* decay and D , b are the diffusion and energy-loss functions respectively. The solution method followed here requires the

approximation that D and b have no positional dependence, such that

$$D(E) = D_0 \left(\frac{d_0}{1 \text{ kpc}} \right)^{\frac{2}{3}} \left(\frac{\bar{B}}{1 \mu\text{G}} \right)^{-\frac{1}{3}} \left(\frac{E}{1 \text{ GeV}} \right)^{\frac{1}{3}}, \quad (4)$$

where $D_0 = 3.1 \times 10^{28} \text{ cm}^2 \text{ s}^{-1}$, d_0 is the magnetic field coherence length, \bar{B} is the average magnetic field strength, and E is the electron energy. The loss-function is found via [11, 18]

$$\begin{aligned} b(E) = & b_{IC} \left(\frac{E}{1 \text{ GeV}} \right)^2 + b_{sync} \left(\frac{E}{1 \text{ GeV}} \right)^2 \left(\frac{\bar{B}}{1 \mu\text{G}} \right)^2 \\ & + b_{Coul} \left(\frac{\bar{n}}{1 \text{ cm}^{-3}} \right) \left(1 + \frac{1}{75} \log \left(\frac{\gamma}{\left(\frac{\bar{n}}{1 \text{ cm}^{-3}} \right)} \right) \right) + b_{brem} \left(\frac{\bar{n}}{1 \text{ cm}^{-3}} \right) \left(\frac{E}{1 \text{ GeV}} \right), \end{aligned} \quad (5)$$

where \bar{n} is the average gas density, the coefficients b_{IC} , b_{sync} , b_{Coul} , b_{brem} are the energy-loss rates from ICS, synchrotron emission, Coulomb scattering, and bremsstrahlung. These coefficients are given by $0.25 \times 10^{-16}(1+z)^4/6.08 \times 10^{-16}$ (for CMB/inter-stellar radiation fields), 0.0254×10^{-16} , 6.13×10^{-16} , 4.7×10^{-16} in units of GeV s^{-1} .

The solution to Eq. (3) when diffusion is negligible is given by [11]

$$\frac{dn_e}{dE} = \frac{1}{b(E)} \int_E^{m_\chi} dE' Q_e(r, E'). \quad (6)$$

When diffusion is not negligible, as in dwarf galaxies like Reticulum II [12, 22], a solution can be found by assuming spherical symmetry [44, 45, 11, 12]

$$\frac{dn_e}{dE}(r, E) = \frac{1}{b(E)} \int_E^{M_\chi} dE' G(r, E, E') Q(r, E'), \quad (7)$$

where this depends upon the Green's function $G(r, E, E')$. This function is expressed as

$$\begin{aligned} G(r, E, E') = & \frac{1}{\sqrt{4\pi\Delta v}} \sum_{n=-\infty}^{\infty} (-1)^n \int_0^{r_h} dr' \frac{r'}{r_n} \\ & \times \left(\exp \left(-\frac{(r' - r_n)^2}{4\Delta v} \right) - \exp \left(-\frac{(r' + r_n)^2}{4\Delta v} \right) \right) \frac{Q(r')}{Q(r)}, \end{aligned} \quad (8)$$

with the sum running over a set of image charges at positions $r_n = (-1)^n r + 2nr_h$, with r_h being the maximum radius of diffusion under consideration. We follow [11] in taking $r_h = 2R_{vir}$ with R_{vir} being the virial radius of the halo in question. Finally, Δv is given by

$$\Delta v = v(u(E)) - v(u(E')), \quad (9)$$

with

$$\begin{aligned} v(u(E)) = & \int_{u_{min}}^{u(E)} dx D(x), \\ u(E) = & \int_E^{E_{max}} \frac{dx}{b(x)}. \end{aligned} \quad (10)$$

2.3. Secondary emissions

As the secondary mechanisms are more complicated than primary ones, we will characterise each process i with an emissivity for frequency ν and halo position r , this being an integral over electron energies E :

$$j_i(\nu, r, z) = \int_{m_e}^{m_{d^*}} dE \left(\frac{dn_{e^-}}{dE}(E, r) + \frac{dn_{e^+}}{dE}(E, r) \right) P_i(\nu, E, r, z) , \quad (11)$$

where $\frac{dn_{e^-}}{dE}$ is the electron distribution within the source region from d^* decay and P_i is the power emitted at frequency ν through mechanism i by an electron with energy E , at position r . The flux produced within a radius r is then found via

$$S_i(\nu, r, z) = \int_0^r d^3r' \frac{j_i(\nu, r', z)}{4\pi(D_L^2 + (r')^2)} . \quad (12)$$

Thus, in order to characterise each mechanism we need only provide the power P_i .

The power produced by the ICS at a photon of frequency ν from an electron with energy E is given by [46, 47]

$$P_{IC}(\nu, E, z) = cE_\gamma(z) \int d\epsilon n(\epsilon) \sigma(E, \epsilon, E_\gamma(z)) , \quad (13)$$

where $E_\gamma(z) = h\nu(1+z)$ with redshift z , ϵ is the energy of the seed photons distributed according to $n(\epsilon)$ (this will taken to be that of the CMB), and

$$\sigma(E, \epsilon, E_\gamma) = \frac{3\sigma_T}{4\epsilon\gamma^2} G(q, \Gamma_e) , \quad (14)$$

with σ_T being the Thompson cross-section and

$$G(q, \Gamma_e) = 2q \ln q + (1+2q)(1-q) + \frac{(\Gamma_e q)^2(1-q)}{2(1+\Gamma_e q)} , \quad (15)$$

with

$$q = \frac{E_\gamma}{\Gamma_e(\gamma m_e c^2 + E_\gamma)} , \quad (16)$$

$$\Gamma_e = \frac{4\epsilon\gamma}{m_e c^2} ,$$

where m_e is the electron mass.

The power from bremsstrahlung at photon energy E_γ from an electron at energy E is given by [46, 47]

$$P_B(E_\gamma, E, r) = cE_\gamma(z) \sum_j n_j(r) \sigma_B(E_\gamma, E) , \quad (17)$$

n_j is the distribution of target nuclei of species j , the cross-section is given by

$$\sigma_B(E_\gamma, E) = \frac{3\alpha\sigma_T}{8\pi E_\gamma} \left[\left(1 + \left(1 - \frac{E_\gamma}{E} \right)^2 \right) \phi_1 - \frac{2}{3} \left(1 - \frac{E_\gamma}{E} \right) \phi_2 \right] , \quad (18)$$

with ϕ_1 and ϕ_2 being energy dependent factors determined by the species j (see [46, 47]).

The power from synchrotron emission at frequency ν from an electron at energy E is given by [47, 46]

$$P_{synch}(\nu, E, r, z) = \int_0^\pi d\theta \frac{\sin \theta}{2} 2\pi \sqrt{3} r_e m_e c \nu_g(r) F_{synch} \left(\frac{\kappa(r)}{\sin \theta} \right), \quad (19)$$

where m_e is the electron mass, $\nu_g(r) = \frac{eB(r)}{2\pi m_e c}$ is the non-relativistic gyro-frequency, $B(r)$ is magnetic field strength at r , $r_e = \frac{e^2}{m_e c^2}$ is the classical electron radius, and the quantities $\kappa(r)$ and F_{synch} are defined as

$$\kappa(r) = \frac{2\nu(1+z)}{3\nu_g(r)\gamma^2} \left[1 + \left(\frac{\gamma\nu_p(r)}{\nu(1+z)} \right)^2 \right]^{\frac{3}{2}}, \quad (20)$$

with the plasma frequency $\nu_p(r) \propto \sqrt{n_e(r)}$ with $n_e(r)$ being the gas density at r , γ as the electron Lorentz factor, and

$$F_{synch}(x) = x \int_x^\infty dy K_{5/3}(y) \approx 1.25 x^{\frac{1}{3}} e^{-x} (648 + x^2)^{\frac{1}{12}}. \quad (21)$$

3. Halo environments and their observed fluxes

With the emission mechanisms now detailed we still require some information to compute the d^* decay flux: namely a d^* density ρ_{d^*} as well as magnetic field and gas profiles, $B(r)$ and $n_e(r)$ respectively, for the decay environment. We choose to study dense DM halos, as if d^* constitutes DM, these will present the strongest signatures due to the scaling of Eq. (2) with ρ_{d^*} . Thus, in this section, we will enumerate the environmental properties of each halo of interest in this work. Furthermore, we will note what observational data will be compared to predicted d^* emissions in order to place limits on the decay rate Γ_{d^*} .

The primary halo characteristic is the DM density profile, entering into flux calculations via Eq. (2). We will make use of the Navarro-Frenk-White (NFW) case [48], the cored Burkert profile [49], and the Einasto profile [50]

$$\begin{aligned} \rho_{nfw}(r) &= \frac{\rho_s}{\left(\frac{r}{r_s} \left(1 + \frac{r}{r_s} \right) \right)^2}, \\ \rho_{burk}(r) &= \frac{\rho_s}{\left(1 + \frac{r}{r_s} \right) \left(1 + \left[\frac{r}{r_s} \right]^2 \right)}, \\ \rho_{ein}(r) &= \rho_s \exp \left[-\frac{2}{\alpha} \left(\left[\frac{r}{r_s} \right]^\alpha - 1 \right) \right], \end{aligned} \quad (22)$$

where α is the Einasto parameter, while r_s and ρ_s are the characteristic halo scale and density respectively. All of these profiles are used under the assumption that the halo is spherically symmetric.

3.1. Coma

In the Coma galaxy cluster we follow [11] in using the halo parameters $M_{vir} = 1.33 \times 10^{15} M_\odot$, $R_{vir} = 1.96$ Mpc, and $r_s = 0.196$ Mpc with an NFW profile (ρ_s is chosen to normalise the density to M_{vir} within R_{vir}).

The gas density within the halo is taken to have a profile

$$n_e(r) = n_0 \left(1 + \left[\frac{r}{r_d} \right]^2 \right)^{-q_e}, \quad (23)$$

with $n_0 = 3.44 \times 10^{-3} \text{ cm}^{-3}$, $q_e = 1.125$, $r_d = 0.29$ Mpc from [33].

The magnetic field model is then

$$B(r) = B_0 \left(\frac{n_e(r)}{n_0} \right)^{q_b}, \quad (24)$$

with $B_0 = 4.7 \text{ } \mu\text{G}$, and $q_b = 0.5$ from [34].

In the Coma galaxy cluster we will compare predicted d^* decay emissions to the diffuse radio data set from [51] and the gamma-ray limits from [9]. The predicted DM flux $S(\nu)$ will be integrated out to the virial radius R_{vir} .

3.2. M31

In M31 we will use an NFW profile with parameters found in [36] to be $M_{vir} = 1.04 \times 10^{12} M_\odot$, $R_{vir} = 0.207$ Mpc, and $r_s = 0.0167$ Mpc (ρ_s is chosen to normalise the density to M_{vir} within R_{vir}). In M31 we use an exponential gas density

$$n_e(r) = n_0 \exp \left(-\frac{r}{r_d} \right), \quad (25)$$

with $n_0 = 0.06 \text{ cm}^{-3}$ [32], and $r_d \approx 5$ kpc fitted in [35]. In this environment we use the magnetic field model from [35] which has, within $r \leq 40$ kpc,

$$B(r) = \frac{4.6 \left(\frac{r_1}{1 \text{ kpc}} \right) + 64}{\left(\frac{r_1}{1 \text{ kpc}} \right) + \left(\frac{r}{1 \text{ kpc}} \right)} \mu\text{G}, \quad (26)$$

with $r_1 = 200$ kpc.

For testing d^* decay predictions in M31 we make use of the radio frequency data set from [13], these are divided into 50' and 15' observing regions (see [13] and references therein for further details). For gamma-rays in M31 we use the data points (but not upper-limits at higher energies) from [52]. We match the integration radius for the DM flux $S(\nu)$ to the region of interest for the data sets we are comparing to.

3.3. Reticulum II

The Reticulum II dwarf galaxy is taken to have a Burkert density profile following arguments from [53, 54]. This profile has $r_s = 0.139$ kpc [14] and is normalised to the annihilation J-factor $8 \times 10^{18} \text{ GeV}^2 \text{ cm}^{-5}$ found in [10] within 0.5° of the galaxy centre.

In Reticulum II we follow [14] in using the profiles for gas density and magnetic field strength:

$$n_e(r) = n_0 \exp\left(-\frac{r}{r_d}\right), \quad (27)$$

and

$$B(r) = B_0 \exp\left(-\frac{r}{r_d}\right). \quad (28)$$

We take r_d to be given by the stellar-half-light radius with a value of 15 pc [55, 56] and we assume $B_0 \approx 1 \mu\text{G}$, $n_0 \approx 10^{-6} \text{ cm}^{-3}$.

In Reticulum II we use, as our observational data, the diffuse flux limit of $12 \mu\text{Jy}$ at 1.873 GHz from [14] and the gamma-ray upper-limits from [10].

3.4. Galactic centre

We use only the gamma-ray spectrum in the galactic centre and so our model data consist of just the annihilation J-factor. This J-factor is defined

$$J(\Delta\Omega) = \int_{\Delta\Omega} \int_{\text{l.o.s}} \rho_{d^*}^2(r(l)) dl d\Omega, \quad (29)$$

where $\Delta\Omega$ is the observed solid angle and l.o.s signifies the line of sight. It is evident that this quantity is equivalent to the integral over r in Eq. (1). We find the J-factor, using CLUMPY [37, 38, 39], to be $9.94 \times 10^{22} \text{ GeV}^2 \text{ cm}^{-5}$ within 10° of the galactic centre, assuming an Einasto halo profile. We normalise our halo profile to the stated J-factor (using the CLUMPY halo parameters) in order to determine the decay products from this target.

In this environment we test the gamma-ray spectrum of the Fermi-LAT excess from [30] against DM predictions using the 10° region of interest around the galactic centre.

4. Results and discussion

The results will be presented in the form of spectra from d^* decay for each target halo. This will be in the form of the flux $E(\nu)S(\nu)$ (calculated as the sum of Eq. (1) and each mechanism from Eq. (12)) which has units of energy per unit area per unit time with $E(\nu) = h\nu$. This will be compared with observational data listed for each halo in section (3). We will display predicted spectra assuming a fiducial value of the d^* decay rate $\Gamma_{d^*} = 10^{-24} \text{ s}^{-1}$. Limits on the actual value of Γ_{d^*} are then derived by requiring that the predicted d^* flux is smaller than the observed flux (as d^* cannot contribute more flux than has already been observed, it could only be responsible for some fraction

of it). Note that Γ_{d^*} being a constant, it acts as a normalisation factor multiplying the calculated spectrum, as displayed in Eq. (2). So the flux for a given Γ_{d^*} is found by multiplying the displayed fiducial fluxes $ES(\nu)$ by $\frac{\Gamma_{d^*}}{10^{-24} \text{ s}^{-1}}$.

The fiducial decay rate is chosen to be similar to the most comparable results in the literature: largely model independent sets from [40, 41] which constrain decaying DM models via direct decay to either photons or electrons and positrons. In our case the most comparable source functions from [40, 41] are those for DM decaying to electrons and positrons, as the spectral shape resembles those found in this work. However, the limits from [40, 41] are not completely compatible with the model from [29]. This is because, while the spectral shapes are somewhat similar, the model-independent gamma-ray yields are around 5 orders of magnitude larger than those presented for the decay of d^* particles. This is due to the fact that d^* decays to e^\pm and photons via intermediate states. So a rough benchmark to compare with our limits derived here will be $\Gamma_{d^*} < 10^{-19} \text{ s}^{-1}$. Additionally, this makes a reasonable benchmark due to the similarity of this $1/\Gamma_{d^*}$ to the age of the universe [1].

Each spectrum has 3 characteristic peaks: one for each of the synchrotron, ICS, and primary emissions (in ascending frequency order). The synchrotron peak falls below 10 MHz and so will not be displayed (as it is likely not visible with Earth-based radio telescopes). The bremsstrahlung contributes the bridging region between ICS and primary peaks. In each case the synchrotron emission dominates spectrum below a few hundred MHz, with the ICS region from 10^3 to 10^{11} MHz, bremsstrahlung between 10^{11} and 10^{15} MHz, and finally primary emissions at higher frequencies. These regions vary slightly between each halo as they depend upon the gas and magnetic field strength profiles through the expressions for mechanism powers in section 2 and also via dependence on electron equilibrium distributions.

In the case of the Coma galaxy cluster in Figure 1 it is evident that existing gamma-ray upper-limits provide the strongest option for constraint in this environment with $\Gamma_{d^*} \leq 7.4 \times 10^{-22} \text{ s}^{-1}$ to avoid exceeding the limits at 2σ confidence interval. This is because of the proximity between these data points and the spectrum plotted with the fiducial decay rate. The observed radio data points are at least 5 orders of magnitude above the predicted spectrum and would thus only be exceeded by the predicted spectrum with a decay rate at least 10^5 times higher than the fiducial value. The resulting constraints from this data are $\Gamma_{d^*} \leq 3.6 \times 10^{-17} \text{ s}^{-1}$. Our results in the Coma case already exceed the model-translated limits from [40, 41] by around 2 orders of magnitude.

M31 results are displayed in Figs. 2 and 3 are also well below the observed data points for the fiducial Γ value. However, the gamma-ray data points from [52] provide a constraint that $\Gamma_{d^*} \leq 1.2 \times 10^{-22} \text{ s}^{-1}$ at the 2σ confidence level. This is vastly better than the Coma cluster radio constraint, and a factor of 6 or so better than the gamma-ray case. Substantially weaker limits result from the radio data points, as opposed to higher energies, largely as the synchrotron emissions peak at such a low frequency as a consequence of the $\sim 2 \text{ GeV } d^*$ mass.

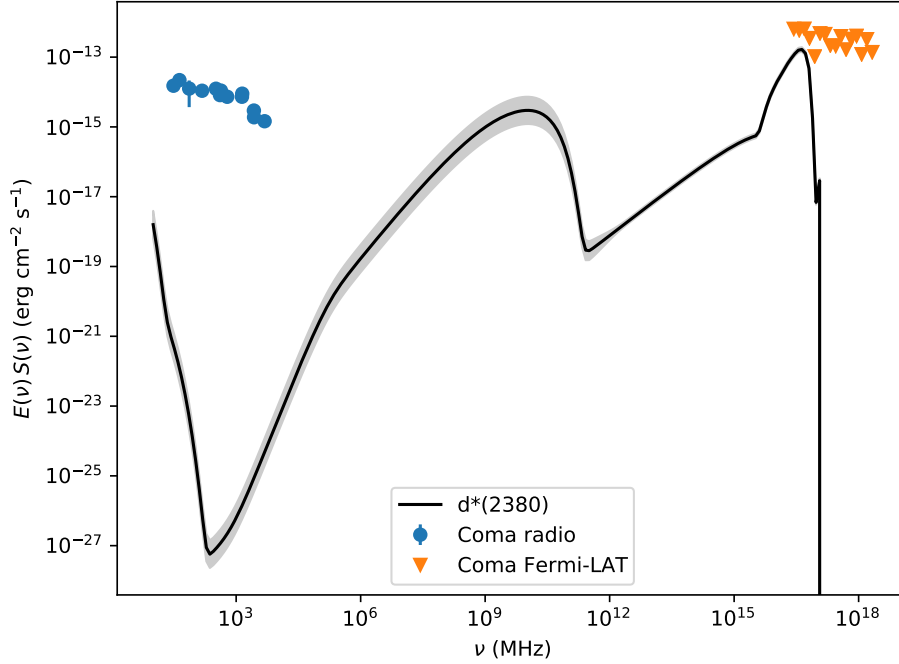


Figure 1. Predicted multi-frequency spectrum from d^* decay in the Coma galaxy cluster with $\Gamma_{d^*} = 10^{-24} \text{ s}^{-1}$. The shaded region indicates uncertainties from the magnetic field and halo mass.

In Figure 4 we display the Reticulum II predicted spectrum. Importantly, the gamma-ray data points do not overlap with the predicted spectrum so can provide no constraints. However, the steep gamma-ray peak suggests that lower energy observations could provide a relatively strong probe of d^* decays in this target. If the power-law trend of the limits is continued, a $\Gamma_{d^*} \leq 10^{-23} \text{ s}^{-1}$ is potentially attainable, bettering even the M31 case. The relatively low energy threshold for ICS dominance in the Reticulum II spectrum also produces surprisingly strong radio limits (given the weak magnetic field assumptions) with $\Gamma_{d^*} \leq 1.04 \times 10^{-14} \text{ s}^{-1}$.

In figure 5 we display the case of the galactic centre gamma-ray spectrum compared to the data from the Fermi-LAT diffuse gamma-ray excess within 10° from [30]. Here we see that the $\Gamma_{d^*} = \times 10^{-24} \text{ s}^{-1}$ case only lies slightly below the observed spectrum and a resulting constraint is that $\Gamma_{d^*} \leq 3.9 \times 10^{-24} \text{ s}^{-1}$, improving on the model translated value from [40, 41] by around 5 orders of magnitude making this competitive even with the unmodified model independent limits.

We present a summary of the constraints on the d^* decay rate Γ_{d^*} in Table 1. These results indicate that the various fluxes from d^* decay are weak but benchmarking against the viability of the hexaquark DM model is difficult without a result for Γ which would be necessary to reproduce the present-day DM abundance. The most optimistic observation case is from our results is the Milky-Way galactic centre which produces limits from gamma-ray fluxes similar to model-independent limits from [40, 40] and 5

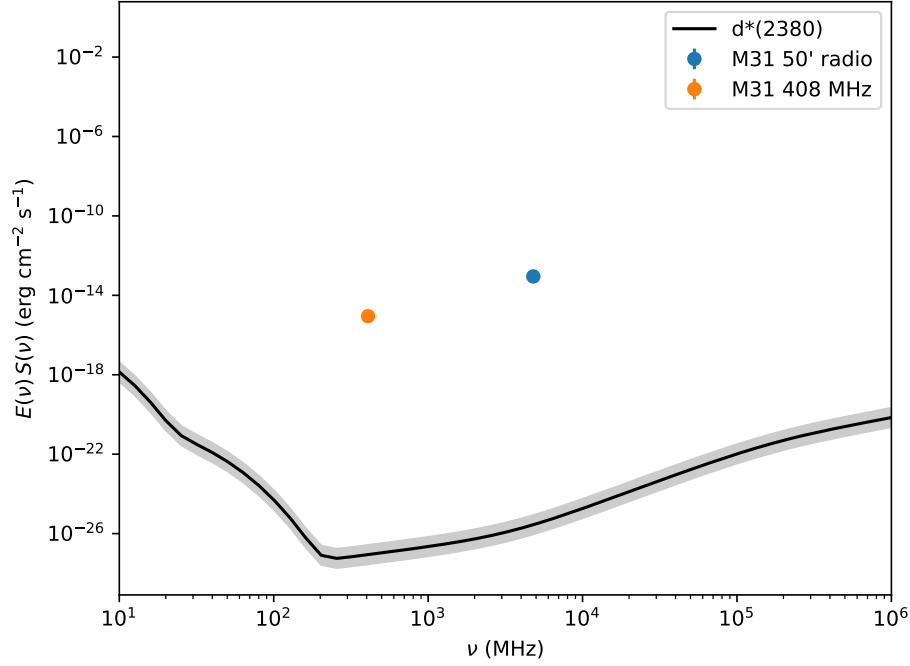


Figure 2. Predicted radio spectrum from d^* decay in the M31 galaxy within $50'$ with $\Gamma_{d^*} = 10^{-24} \text{ s}^{-1}$. The shaded region indicates uncertainties from the magnetic field and halo mass.

Data set	Limit
GC gamma-ray	$\Gamma_{d^*} \leq 3.9 \times 10^{-24} \text{ s}^{-1}$
M31 gamma-ray	$\Gamma_{d^*} \leq 1.2 \times 10^{-22} \text{ s}^{-1}$
Coma gamma-ray	$\Gamma_{d^*} \leq 7.4 \times 10^{-22} \text{ s}^{-1}$
Coma radio	$\Gamma_{d^*} \leq 3.6 \times 10^{-17} \text{ s}^{-1}$
Reticulum II radio	$\Gamma_{d^*} \leq 1.04 \times 10^{-14} \text{ s}^{-1}$
M31 radio	$\Gamma_{d^*} \leq 4.9 \times 10^{-14} \text{ s}^{-1}$

Table 1. Summary of 2σ confidence interval limits on the d^* decay rate in different DM halos.

orders of magnitude better than the roughly translated model-dependent value 10^{-19} s^{-1} . Despite being two orders of magnitude smaller than Γ_{d^*} limits from the galactic centre, M31 and Coma still provide limits $\Gamma_{d^*} \lesssim 10^{-22} \text{ s}^{-1}$, indicating a particle lifetime lower limit around two orders of magnitude in excess of the age of the universe. If not for the limited energy range of the Reticulum II gamma-ray data it is likely that the strongest extra-galactic environment for these constraints is dwarf galaxies (particularly with gamma-ray measurements or perhaps millimetre telescopes). Radio limits are weak across the board due to the very low energy of the synchrotron peak as a consequence of the small d^* mass. Particularly, this synchrotron peak lies below 10 MHz and is therefore likely unobservable within the atmosphere of Earth.

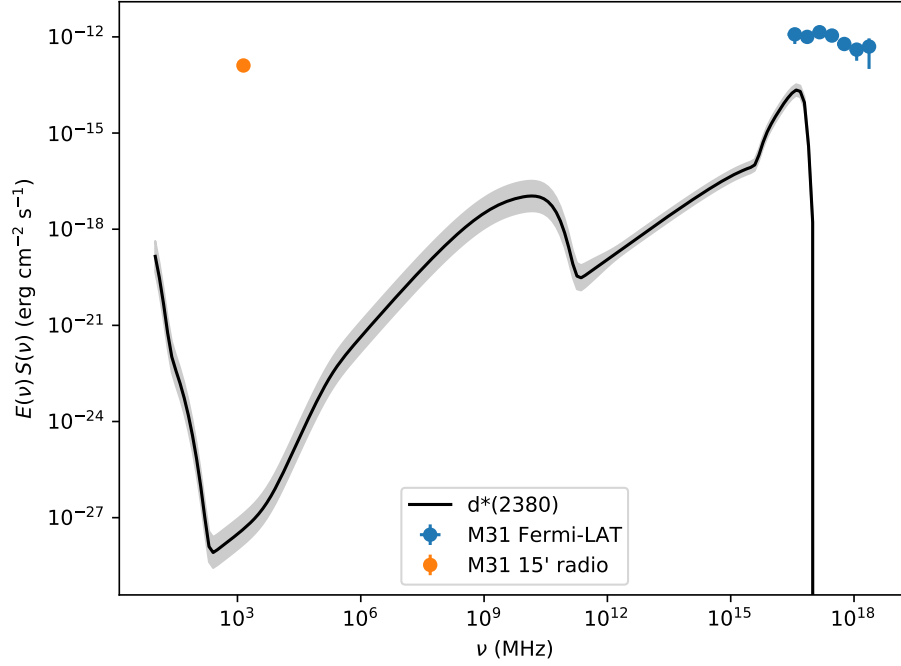


Figure 3. Predicted multi-frequency spectrum from d^* decay in the M31 galaxy within 15' with $\Gamma_{d^*} = 10^{-24} \text{ s}^{-1}$. The shaded region indicates uncertainties from the magnetic field and halo mass.

5. Summary and conclusions

We have presented a comparison of emission predictions from the decay of d^* hexaquark particles to observed multi-frequency spectra in M31, the Milky-Way galactic centre, Reticulum II, and the Coma galaxy cluster. These results were used to place the first limits on the decay rate of the d^* particle and explore the suggestion in [29] that indirect astrophysical observations would provide the strongest signatures of d^* BEC DM. Our findings were that the best limit on the decay rate is found in the Milky-Way galactic centre with $\Gamma_{d^*} \leq 3.9 \times 10^{-24} \text{ s}^{-1}$ by comparing predicted spectra to the Fermi-LAT excess spectrum from [30].

Since this DM model has not been probed indirectly before it is not trivial to compare to existing literature. This is because any relevant limits will have to be sourced from model independent studies. The results most comparable to our work yield $\Gamma \leq \times 10^{-24} \text{ s}^{-1}$ [40, 41] for light DM (with similar mass to d^*) decaying into e^\pm directly. This approach results in a similar spectral shape to ours but over-produces the d^* photon spectrum by a factor of 10^5 . Thus, our results are comparable to existing model-independent limits at face value but also greatly exceed a ‘model adjusted’ version of the [40] limit at $\Gamma \leq \times 10^{-19} \text{ s}^{-1}$. The discrepancy between the model independent case and that of d^* arises because d^* decays produce stable particles via initial decay to pions, rather than the direct production explored in the model independent literature in question.

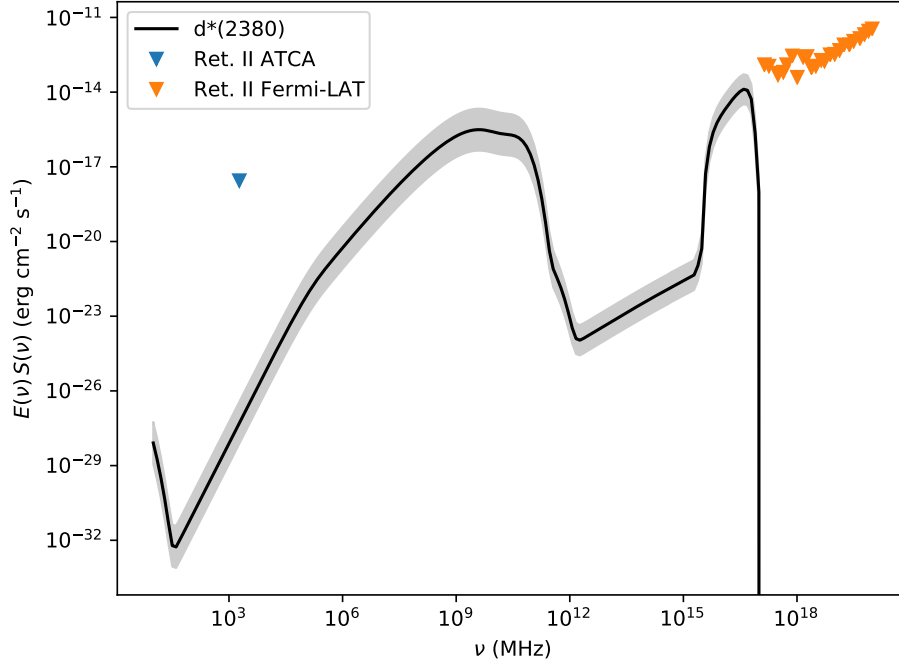


Figure 4. Predicted multi-frequency spectrum from d^* decay in the Reticulum II dwarf galaxy within $30'$ with $\Gamma_{d^*} = 10^{-24} \text{ s}^{-1}$. The shaded region indicates uncertainties from the magnetic field and halo mass.

The uncertainties from halo parameters in the presented results are notably small in comparison to the difference with the lower limits from [40] (model independent limits on decaying DM) and tend to be smaller in the simpler gamma-ray region of the spectrum. However, unquantified uncertainties exist in terms of the required Γ value to achieve a significant present-day DM fraction and in the formalism used to convert charged pion products to electrons/positrons (as the quantitative effect of the neglected radiative corrections is unknown). This latter uncertainty does not affect the gamma-ray results as they were all attained from the neutral pion decay channels of d^* .

Despite these uncertainties it seems likely that the emissions from d^* hexaquark decay produce relatively weak fluxes in astrophysical environments but that gamma-ray searches in galaxy clusters, galaxies, and dwarf galaxies at energies below 1 GeV may be able to provide further constraints. The data used in this work was not optimised for this kind of indirect DM search so the results produced could undoubtedly be improved upon in the future. One possible improvement in methodology would be to disentangle the constituents of decay rate (as described in section 2) in order to produce limits on the d^* -cosmic-ray interaction cross-section.

Acknowledgements

G.B acknowledges support from a National Research Foundation of South Africa Thuthuka grant no. 117969. This research has made use of the NASA/IPAC

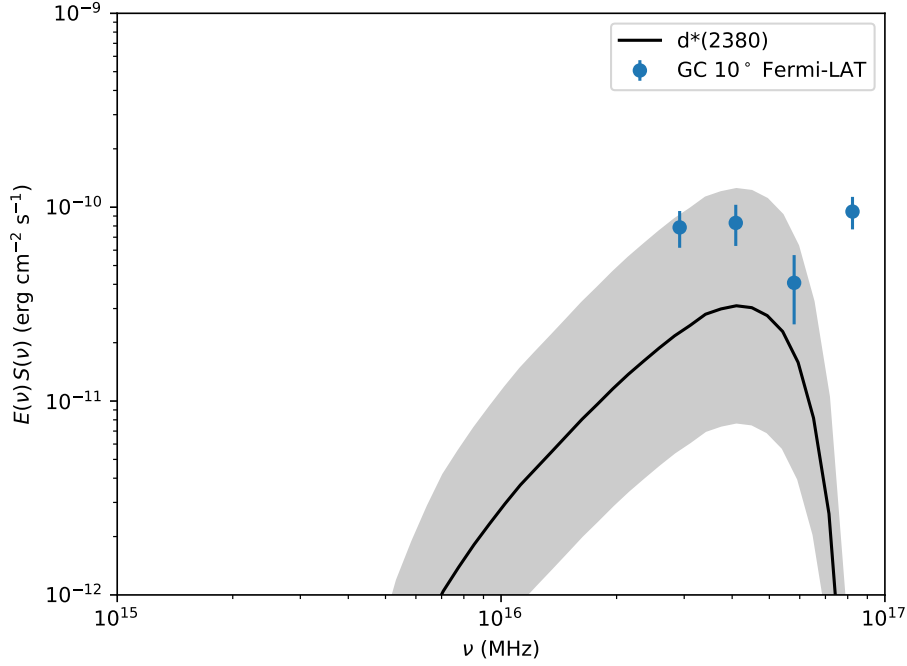


Figure 5. Predicted multi-frequency spectrum from d^* decay within 10° of the Milky-Way galactic centre with $\Gamma_{d^*} = 10^{-24} \text{ s}^{-1}$. The shaded region indicates uncertainties from the halo J-factor.

Extragalactic Database (NED), which is operated by the Jet Propulsion Laboratory, California Institute of Technology, under contract with the National Aeronautics and Space Administration. This work also made use of the WebPlotDigitizer[‡].

- [1] Aghanim N *et al.* (Planck Collaboration) 2018 (*Preprint* 1807.06209)
- [2] Koopmans L V E and Treu T 2003 *The Astrophysical Journal* **583** 606615 ISSN 1538-4357 URL <http://dx.doi.org/10.1086/345423>
- [3] Metcalf R B, Moustakas L A, Bunker A J and Parry I R 2004 *The Astrophysical Journal* **607** 4359 ISSN 1538-4357 URL <http://dx.doi.org/10.1086/383243>
- [4] Hoekstra H, Yee H and Gladders M D 2002 *New Astronomy Reviews* **46** 767781 ISSN 1387-6473 URL [http://dx.doi.org/10.1016/S1387-6473\(02\)00245-2](http://dx.doi.org/10.1016/S1387-6473(02)00245-2)
- [5] Moustakas L A and Metcalf R B 2003 *Monthly Notices of the Royal Astronomical Society* **339** 607615 ISSN 1365-2966 URL <http://dx.doi.org/10.1046/j.1365-8711.2003.06055.x>
- [6] Bertone G and Tait Tim M P 2018 *Nature* **562** 51–56 (*Preprint* 1810.01668)
- [7] Aprile E *et al.* (XENON Collaboration 7) 2018 *Phys. Rev. Lett.* **121**(11) 111302 URL <https://link.aps.org/doi/10.1103/PhysRevLett.121.111302>
- [8] Schumann M 2019 *Journal of Physics G: Nuclear and Particle Physics* **46** 103003 ISSN 1361-6471 URL <http://dx.doi.org/10.1088/1361-6471/ab2ea5>
- [9] Ackermann M *et al.* (Fermi-LAT Collaboration) 2016 *The Astrophysical Journal* **819** 149 ISSN 1538-4357 URL <http://dx.doi.org/10.3847/0004-637X/819/2/149>
- [10] Albert A *et al.* (Fermi-LAT and DES Collaborations) 2017 *The Astrophysical Journal* **834** 110 ISSN 1538-4357 URL <http://dx.doi.org/10.3847/1538-4357/834/2/110>
- [11] Colafrancesco S, Profumo S and Ullio P 2006 *A&A* **455** 21
- [12] Colafrancesco S, Profumo S and Ullio P 2007 *Phys. Rev. D* **75** 023513

[‡] <http://automeris.io/WebPlotDigitizer/>

- [13] Beck G 2019 *JCAP* **1908** 019 (*Preprint* 1905.05599)
- [14] Regis M, Richter L and Colafrancesco S 2017 *Journal of Cosmology and Astroparticle Physics* **2017** 025 URL <http://stacks.iop.org/1475-7516/2017/i=07/a=025>
- [15] Chan M H, Cui L, Liu J and Leung C S 2019 *The Astrophysical Journal* **872** 177 ISSN 1538-4357 URL <http://dx.doi.org/10.3847/1538-4357/aafe0b>
- [16] Chan M H 2017 *Phys. Rev.* **D96** 043009 (*Preprint* 1708.01370)
- [17] Abdallah H *et al.* (H.E.S.S.) 2016 *Phys. Rev. Lett.* **117** 111301 (*Preprint* 1607.08142)
- [18] Egorov A E and Pierpaoli E 2013 *Phys. Rev. D* **88** 023504 (*Preprint* 1304.0517)
- [19] Caputo R, Buckley M R, Martin P, Charles E, Brooks A M, Drlica-Wagner A, Gaskins J and Wood M 2016 *Phys. Rev. D* **93**(6) 062004 URL <https://link.aps.org/doi/10.1103/PhysRevD.93.062004>
- [20] Siffert B B, Limone A, Borriello E, Longo G and Miele G 2011 *Monthly Notices of the Royal Astronomical Society* **410** 2463–2471 (*Preprint* 1006.5325)
- [21] Storm E, Jeltema T E, Splettstoesser M and Profumo S 2017 *The Astrophysical Journal* **839** 33 URL <http://stacks.iop.org/0004-637X/839/i=1/a=33>
- [22] Beck G and Colafrancesco S 2016 *JCAP* **1605** 013 (*Preprint* 1508.01386)
- [23] Beck G 2019 *Journal of Cosmology and Astroparticle Physics* **2019** 019019 ISSN 1475-7516 URL <http://dx.doi.org/10.1088/1475-7516/2019/08/019>
- [24] Boyarsky A, Drewes M, Lasserre T, Mertens S and Ruchayskiy O 2019 *Progress in Particle and Nuclear Physics* **104** 145 ISSN 0146-6410 URL <http://dx.doi.org/10.1016/j.pnpnp.2018.07.004>
- [25] Duffy L D and Bibber K v 2009 *New Journal of Physics* **11** 105008 ISSN 1367-2630 URL <http://dx.doi.org/10.1088/1367-2630/11/10/105008>
- [26] Graham P W, Irastorza I G, Lamoreaux S K, Lindner A and van Bibber K A 2015 *Annual Review of Nuclear and Particle Science* **65** 485–514 (*Preprint* <https://doi.org/10.1146/annurev-nucl-102014-022120>) URL <https://doi.org/10.1146/annurev-nucl-102014-022120>
- [27] Anastassopoulos V *et al.* (CAST) 2017 *Nature Physics* **13** 584590 ISSN 1745-2481 URL <http://dx.doi.org/10.1038/nphys4109>
- [28] Braine T, Cervantes R, Crisosto N, Du N, Kimes S, Rosenberg L, Rybka G, Yang J, Bowring D, Chou A and *et al* 2020 *Physical Review Letters* **124** ISSN 1079-7114 URL <http://dx.doi.org/10.1103/PhysRevLett.124.101303>
- [29] Bashkanov M and Watts D P 2020 *Journal of Physics G: Nuclear and Particle Physics* **47** 03LT01 URL <https://doi.org/10.1088/2F1361-6471/2Fab67e8>
- [30] Ackermann M, Ajello M, Albert A, Atwood W B, Baldini L, Ballet J, Barbiellini G, Bastieri D, Bellazzini R, Bissaldi E and *et al* 2017 *The Astrophysical Journal* **840** 43 ISSN 1538-4357 URL <http://dx.doi.org/10.3847/1538-4357/aa6cab>
- [31] Bonnivard V, Combet C, Maurin D, Geringer-Sameth A, Koushiappas S M, Walker M G, Mateo M, Olszewski E W and Bailey III J I 2015 *Astrophys. J.* **808** L36 (*Preprint* 1504.03309)
- [32] Beck R 1982 *A&A* **106** 121
- [33] Briel U G, Henry J P and Boehringer H 1992 *Astronomy and Astrophysics* **259** L31–L34
- [34] Bonafede A, Feretti L, Murgia M, Govoni F, Giovannini G, Dallacasa D, Dolag K and Taylor G B 2010 *Astronomy and Astrophysics* **513** A30 ISSN 1432-0746 URL <http://dx.doi.org/10.1051/0004-6361/200913696>
- [35] Ruiz-Granados B, Rubiño-Martín J A, Florido E and Battaner E 2010 *ApJ* **723** L44–L48 URL <https://doi.org/10.1088/2F2041-8205/2F723/2F1/2F144>
- [36] Tamm A, Tempel E, Tenjes P, Tihhonova O and Tuvikene T 2012 *A&A* **546** A4 (*Preprint* 1208.5712)
- [37] Charbonnier A, Combet C and Maurin D 2012 *Computer Physics Communications* **183** 656668 ISSN 0010-4655 URL <http://dx.doi.org/10.1016/j.cpc.2011.10.017>
- [38] Bonnivard V, Htten M, Nezri E, Charbonnier A, Combet C and Maurin D 2016 *Computer Physics*

- Communications* **200** 336349 ISSN 0010-4655 URL <http://dx.doi.org/10.1016/j.cpc.2015.11.012>
- [39] Hütten M, Combet C and Maurin D 2019 *Computer Physics Communications* **235** 336–345 (*Preprint* 1806.08639)
 - [40] Essig R, Kuflik E, McDermott S D, Volansky T and Zurek K M 2013 *JHEP* **11** 193 (*Preprint* 1309.4091)
 - [41] Liu H, Slatyer T R and Zavala J 2016 *Physical Review D* **94** ISSN 2470-0029 URL <http://dx.doi.org/10.1103/PhysRevD.94.063507>
 - [42] Scanlon J H and Milford S N 1965 *ApJ* **141** 718
 - [43] Gal A 2019 *EPJ Web Conf.* **199** 02018
 - [44] Baltz E A and Edsjö J 1998 *Phys. Rev. D* **59**(2) 023511 URL <https://link.aps.org/doi/10.1103/PhysRevD.59.023511>
 - [45] Baltz E A and Wai L 2004 *Phys. Rev. D* **70**(2) 023512 URL <https://link.aps.org/doi/10.1103/PhysRevD.70.023512>
 - [46] Longair M S 1994 *High Energy Astrophysics* (Cambridge University Press)
 - [47] Rybicki G B and Lightman A P 1986 *Radiative Processes in Astrophysics* (Wiley)
 - [48] Navarro J F, Frenk C S and White S D M 1996 *Astrophys. J.* **462** 563–575 (*Preprint* astro-ph/9508025)
 - [49] Burkert A 1996 *IAU Symp.* **171** 175 [*Astrophys. J.*447,L25(1995)] (*Preprint* astro-ph/9504041)
 - [50] Einasto J 1968 *Publications of the Tartuskoj Astrofizica Observatory* **36** 414
 - [51] Thierbach M, Klein U and Wielebinski R 2003 *A&A* **397** 53
 - [52] Ackermann M *et al.* (Fermi-LAT Collaboration) 2017 *The Astrophysical Journal* **836** 208 URL <https://doi.org/10.3847/2F1538-4357/2Faa5c3d>
 - [53] Walker M G, Mateo M, Olszewski E W, narrubia J P, Evans N W and Gilmore G 2009 *ApJ* **704** 1274 URL <http://stacks.iop.org/0004-637X/704/i=2/a=1274>
 - [54] Adams J J *et al.* 2014 *ApJ* **789** 63 URL <http://stacks.iop.org/0004-637X/789/i=1/a=63>
 - [55] Bechtol K *et al.* (DES Collaboration) 2015 *ApJ* **807** 50 (*Preprint* 1503.02584)
 - [56] Koposov S E, Belokurov V, Torrealba G and Evans N W 2015 *ApJ* **805** 130 (*Preprint* 1503.02079)